View metadata, citation and similar papers at core.ac.uk

brought to you by CORE

provided by Elsevier - Publisher Connector

Available online at www.sciencedirect.com

ScienceDirect

Procedia Engineering 62 (2013) 182 – 193

Procedia Engineering

www.elsevier.com/locate/procedia

The 9th Asia-Oceania Symposium on Fire Science and Technology

Combustion chemistry and decomposition kinetics of forest fuels

Oleg P. Korobeinichev[a,*], Alexander A. Paletsky[a], Munko B. Gonchikzhapov[a,b], Inna K. Shundrina[c], Haixiang Chen[d], Naian Liu[d]

[a]*Institute of Chemical Kinetics and Combustion, Novosibirsk 630090, Russia*
[b]*Novosibirsk State University, Novosibirsk 630090, Russia*
[c]*Novosibirsk Institute of Organic Chemistry, Novosibirsk 630090, Russia*
[d]*State Key Laboratory of Fire Science, University of Science and Technology of China, Hefei 230026, China*

Abstract

A brief review is given of the studies in combustion chemistry and decomposition kinetics of forest fuels (FF). The methods used in the study to investigate the FF pyrolysis kinetics and the combustion of the Siberian forests are described. The experiments on FF pyrolysis were conducted at high heating rates (150 K/s) in a flow reactor by the method of differential mass-spectrometric thermal analysis (DMSTA) *in situ* using probe molecular-beam mass spectrometry, and at low heating rates (0.17 K/s) by the thermogravimetric method. The kinetic parameters of Siberian FF pyrolysis have been determined for oxidative and inert media and simulation of FF pyrolysis has been conducted using the multi-component devolatilization mechanism. The flame structure of a pine branch has been studied by probe molecular-beam mass spectrometry. Species have been identified in the dark and luminous flame zones; the width of the flame zone has been measured.

© 2013 International Association for Fire Safety Science. Published by Elsevier Ltd. Open access under CC BY-NC-ND license.
Selection and peer-review under responsibility of the Asian-Oceania Association of Fire Science and Technology

Keywords: Forest fuels; Pyrolysis kinetics; Differential mass-spectrometric thermal analysis; Flame structure; Forest fire; Probing molecular-beam mass-spectrometry; Thermogravimetric analysis

Nomenclature

FF	forest fuels
PB	pine bark
PN	pine needle
PBr	branches without needles
DMSTA	differential mass-spectrometric thermal analysis
TG/DSC	thermal gravimetry / differential scanning calorimetry
GC/MS	gas chromatography / mass spectrometry
DTG	differential thermal gravimetry

1. Introduction

The combustion processes as such and the combustion processes of forest fuels (FF) are controlled both by chemical reactions, as a rule resulting in heat release, and the processes of heat and mass exchange. Chemical processes play a major role in FF combustion and in the flash and spread of forest fires. The most important chemical stages are: 1). FF pyrolysis, proceeding in several phases to form volatile products (pyrolysates) and condensed carbonaceous residue (char). As a rule,

* Corresponding author. Tel.: +7 383 333 2852; fax: +7 383 330 7350.
E-mail address: korobein@kinetics.nsc.ru

1877-7058 © 2013 International Association for Fire Safety Science. Published by Elsevier Ltd. Open access under CC BY-NC-ND license.
Selection and peer-review under responsibility of the Asian-Oceania Association of Fire Science and Technology
doi:10.1016/j.proeng.2013.08.054

pyrolysis products consist of H_2O, CO, CO_2 and light hydrocarbons – CH_4, C_2H_2, C_2H_4, C_2H_6, C_3H_6, etc. 2). Gas phase oxidation reactions of volatile pyrolysis products with air oxygen in diffusion flame, resulting in the formation of CO_2 and H_2O and heat release. 3). Heterogeneous reactions of char oxidation with air oxygen. The first stage of pyrolysis of FF, which usually contains 10-12% moisture, involves drying of the biomass yielding dry product and water vapors. The rate and the mechanism of dry FF pyrolysis depend on the medium (inert or oxidative) in which it occurs. In air, the pyrolysis rate is higher and the composition of the pyrolysis products changes. A great variety of FF should be born in mind, different for their chemical composition. The composition of FF is complex, containing hemi-cellulose, cellulose, lignin, and other components. This determines the variety of the kinetic processes taking place in FF.

The knowledge of the kinetics and the mechanism of FF pyrolysis is a necessary condition for developing an adequate model of FF combustion, a model of the flash and spread of forest fires. However, model development is essentially slowed down by the lack of both reliable experimental data on the kinetics and mechanism of FF pyrolysis and by the need for a correct method of their processing with the required kinetic parameters obtained. An important step in finding the kinetic parameters of FF pyrolysis, such as the reaction order, the pre-exponential factor, the activation energy, is to establish the mechanism of FF pyrolysis, the pyrolysis model. In a general case, the process of FF combustion may consist of parallel and consecutive stages. In literature, there are numerous studies dedicated to investigating the kinetics and the mechanism of FF pyrolysis and pyrolysis of their components in inert and oxidative media [1-15]. In [1, 2], the multi-stage models of FF pyrolysis are considered. In [1], a model of oxidative FF pyrolysis is examined, consisting of four stages:

$$\text{wet wood} \rightarrow \nu_{dw}\text{dry wood} + \nu_{H2O}\,H_2O$$

$$\text{dry wood} \rightarrow \nu_{char}\text{char} + \nu_{tp}\text{thermal pyrolysate}$$

$$\text{dry wood} + \nu_{O2dw}O_2 \rightarrow \nu_{char}\text{char} + \nu_{op}\text{oxidative pyrolysate}$$

$$\text{char} + \nu_{O2char}\text{O2} \rightarrow \nu_{ash}\text{ash} + \nu_{cop}\text{char oxidation products}$$

Here wet wood stands for wet FF, dry wood is dry FF, thermal pyrolysate is the product of thermal pyrolysis of FF, oxidative pyrolysate is the product of oxidative pyrolysis of FF, with char and char oxidation products being what they are. In [1], oxidation reactions of volatile products of thermal and oxidative FF pyrolysis with oxygen are considered. The pyrolysis models in inert and oxidative media for pine needles (5 stages) and that for cones (4 stages) are considered in [2]. The kinetics of thermal decomposition of FF (pine, aspen, birch, oak) in inert and oxidative media is examined in [3, 4]. In [5], four stages of pine needles pyrolysis are determined (including the drying stage). For each of the stages, the kinetic parameters – the reaction order and the pre-exponential factor are determined for the heating rates varying from 5 to 30 K/min. In [6], the combustion kinetics of pine needles is studied and, in supposition of a two-stage pyrolysis process, the kinetic parameters of this process are determined. In [7], the kinetics of FF combustion of eight different types of wood and leaves in air has been experimentally studied. To describe the kinetics of the forest fuels under study, the authors suggested a "pseudo-two component model of the first order with separate stages", in which the pyrolysis process is supposed to consist of three stages. It is to be noted that the number of papers dedicated to the study of the kinetics of FF pyrolysis, mostly of the forests of the Mediterranean and other western European regions, is rather large. Among these works, the majority of papers are dedicated to the study of the pyrolysis kinetics of pine needles and cones, which are widespread in the Mediterranean region, by the methods of thermal gravimetry and differential scanning calorimetry, and of the composition of the pyrolysis products with infrared Fourier spectroscopy and chromato-mass-spectrometry. Analysis has shown that there are few data [8] on the FF pyrolysis kinetics of Siberian forests. The kinetics and the mechanism of FF pyrolysis are being actively studied not only in connection with forest fires but also with possible application of the pyrolysis of organic materials (mostly lumber waste) to the production of biofuels [9-12]. In [13], the results and a review of studies are presented for the kinetics and the chemical mechanism of cellulose pyrolysis in inert medium, cellulose being one of the major components of FF (~50 wt%). In supposition of the first-order reaction, the kinetic parameters of cellulose pyrolysis were obtained. It was also shown in the paper that, in the range of cellulose heating rates from 1 to 150 K/min, the pyrolysis kinetics does not change. According to the literary data, pine wood consists of ~16 %wt. hemi-cellulose, ~52% cellulose, ~28% lignin and ~4% inorganic materials. The chemical composition of pinewood corresponds to the following ratio: C:H:O 1:1.29:0.72. In [14], in supposition of the first-order reaction, the activation energy of the first stage of pinewood decomposition in the range of the heating rates from 10 to 100 K/min was found to vary between 112 and 125 kJ/mol. The activation energy of the second stage decreases from 145 to 80 kJ/mol with the increase of the heating rate from 10 to 100 K/min. In [15], the FF combustion rate in oxidative medium was established to depend weakly on air concentration.

The results obtained for low heating rates may be applied only for description of smoldering of a forest floor. As shown by the literature review, the kinetic of thermal decomposition of FF at a high heating rate has been poorly investigated. In

this regard, the goal of this study is to investigate and compare thermal decomposition of FF at significantly differing heating rates.

2. Materials

The materials under study were FF collected in the coniferous forests of Siberia, representing the pine (*Pínus sylvéstris*) parts fallen onto the ground (fall) as: 1) bark from the tree stem (PB), 2) pine needles (PN) and 3) branches without needles (PBr). The studies were conducted of FF powder with the characteristic particle size: PB~ 0.17-0.40 mm, PN ~ 0.1-0.3 mm wide and 0.3-1 mm long, Br ~ 0.15-0.48 mm. The FF moisture level corresponded to the air moisture (relative air moisture ~ 40-50%) with the air temperature being 18-22 °C. The specimens were ground in a mortar, then they were ground into powder in a coffee-grinder and sifted. The forest fuel powder samples were not dried prior to experiments.

3. The experimental technique

3.1. Differential mass-spectrometric thermal analysis

Thermal decomposition at a high heating rate of the FF powders under study was carried out in a flow reactor by the method of differential mass-spectrometric thermal analysis (DMSTA) [16]. The DMSTA method is an effective method of studying the kinetics and the mechanism of thermal decomposition of condensed systems and has been successfully used in studying combustion of coals [17], polymers [18], and condensed energy materials [19, 20].

The flow reactor [19] was a quartz tube with a 1 cm diameter, along which the carrier gas (air/argon) flows. Inside the tube was a steel trough, which was heated as electric current was applied to it. The heating rate was ~100-200 K/s. The trough temperature was controlled with a chromel-copel thermocouple welded to its center. Place into the trough was a sample of the powder under study weighing ~0.2-0.4 mg. The sample was analyzed by the method of probing molecular-beam TOF mass-spectrometry (electron impact, 70 eV). The distance between the trough and the orifice of the quartz probe was ~ 3 mm.

3.2. Thermogravimetric analysis

Thermal decomposition at a low heating rate was conducted in a synchronous TG/DSC analyzer STA 409 PC (Netzsch) at different heating rates (10, 20, 30, 40 and 50 K/min) in inert (helium) and oxidative (helium / 21% oxygen) media. The sample weight was 4 mg.

3.3. Investigating combustion of a pine branch

The structure of the diffusion flame of a pine branch was studied by the method of probing molecular-beam mass-spectrometry applied to flames of condensed systems, described in [18]. To identify the combustion products, the method of GC/MS was also used. The burning rate was measured by analyzing the video recording. The video of the combustion process was recorded with a Panasonic M3000 camera.

4. The kinetic model

4.1. The kinetic model of FF pyrolysis at a high heating rate

The main feature of the DMSTA method consists in the fact that the intensity peaks I_i in the mass spectrum of a sample taken at the output of a reactor are directly proportional to the rates of evolution of the respective decomposition products W_i:

$$W_i = W_{Ar} \frac{I_i}{I_{Ar}} \frac{1}{K_i}$$

where K_i is the calibration coefficient; I_{Ar}, W_{Ar} are the mass peak intensity and the flow rate of the argon diluent. Simultaneous measurements of the dependence of the specimen temperature and the mass peak intensities of the decomposition products on time allow the decomposition kinetics to be studied. Analysis of the kinetic data was conducted in supposition of the first-order reaction by the techniques described in [19].

4.2. *The kinetic model of FF pyrolysis at a low heating rate*

Reference [20] describes a method used to process the experimental data of thermogravimetric analysis. The method applies different heating rates to determine the reaction order and the activation energy as a function of the degree of substance transformation.

5. Results

5.1. Thermogravimetric analysis of FF decomposition in oxidative and inert media

Shown in Fig. 1 are the TGA data for pine bark at 5 heating rates 10, 20, 30, 40 and 50 K/min in helium medium and in the helium/oxygen (21 %) mixture. For other FF, the respective dependences were of a similar character. As can be seen, incomplete decomposition is observed for FF decomposition in inert medium.

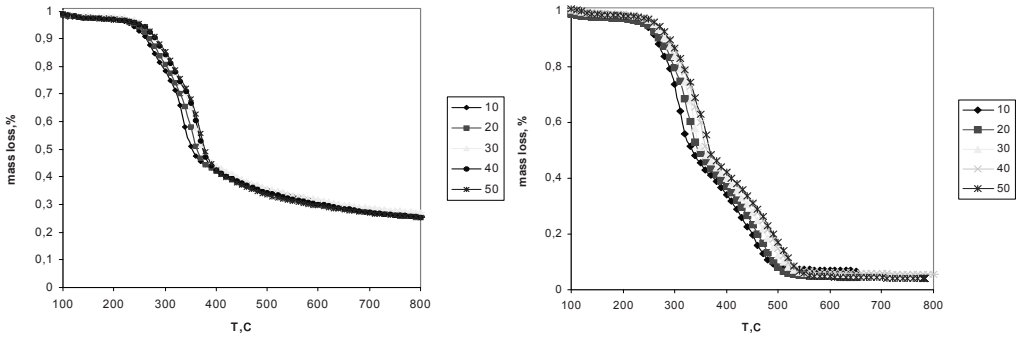

Fig 1. Thermogravimetric curves TG for pine bark in helium (left) and in the helium / 21% oxygen mixture (right).

Based on the data obtained and using the method described in [20], dependences of the rate constant and of the activation energy of thermal decomposition of FF (pine branches, bark and needles) on the degree of decomposition in inert and oxidative media were computed. The computation results are shown in Fig. 2. Table 1 represents the kinetic parameters of the process of decomposition of the FF under study in inert and oxidative media. As seen, the activation energies under thermal decomposition in oxidative medium are lower than those under decomposition in inert medium.

Table 1. Kinetic parameters of the thermal decomposition reaction for FF

TGA	Helium			Helium/oxygen		
	α	$\log k_0$ (1/s)	E_a (kJ/mol)	α	$\log A_0$ (1/s)	E_a (kJ/mol)
Pine branches	[0.04..0.56]	10.6	167.6	[0.02..0.49]	5.8	89
				[0.6..0.9]		133.8
Pine bark	[0.04..0.52]	12	184.3	[0.02..0.49]	6.4	22.6
				[0.6..0.9]		94.5
Pine needles	[0.1..0.6]	10.2	164.3	[0.001..0.5]	6.3	89.9
				[0.7..0.9]		131.7

Figure 3 on the left shows TG, DTG and DSC data for decomposition of pine needles (PN) in inert (helium) and oxidative (79%He+21%O_2) media at the heating rate of 40 K/min. In inert medium decomposition of PN was incomplete and proceeds in one stage (line DTG_{in}) actually without heat release. At the temperature of 700 °C, the fraction of the undecomposed matter (char) was about 20% of the initial mass. At the temperature of ~380 °C, at the maximum decomposition rate of PN in inert medium, the loss of mass was 50%. In oxidative medium, decomposition of PN occurs in two stages (line DTG_{ox}) with heat released at each stage, with much more heat released at the second stage (oxidation of char) than at the second one. The decomposition rates at the first stage in oxidative and inert media were close; however, the

peak value of PN decomposition in the oxidative medium was at a higher temperature than in the inert medium. The second stage of PN decomposition in oxidative medium proceeded in the range of temperatures between 400 °C and 600 °C.

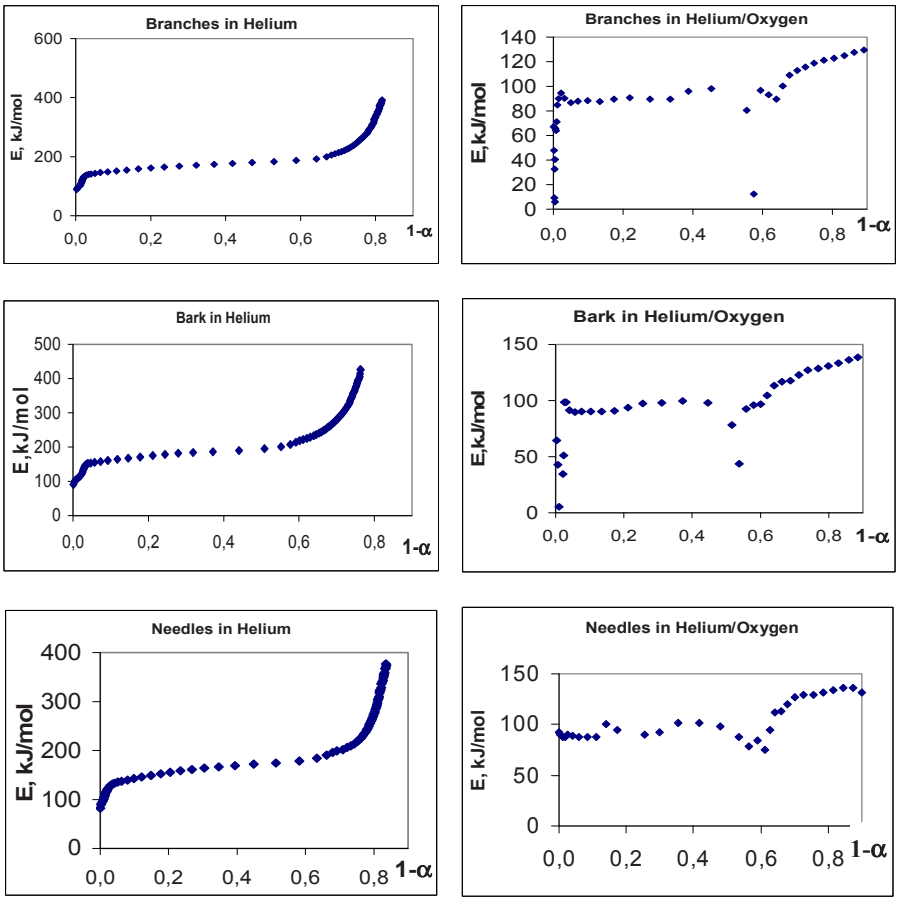

Fig. 2. Dependences of the activation energy on the degree of FF decomposition.

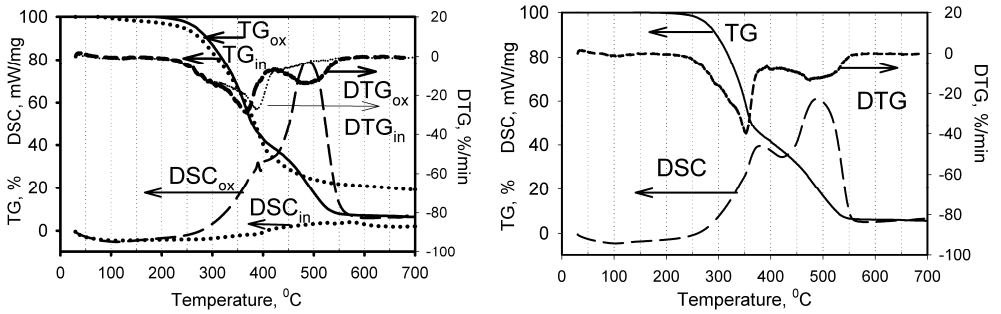

Fig. 3. TG, DTG, DSC decomposition of pine needles (left) in oxidative (79% He+21% O_2) medium (ox-subindex) and in inert medium (in-subindex) and of pine branches in oxidative medium (right) at the heating rate of 40 K/min.

Figure 3 (right) shows similar data according to TG, DTG, and DSC for decomposition of pine branches (PBr) in oxidative medium (79% He+21% O_2) at the heating rate of 40 K/min. The general course of the curves is similar for PN and PBr; however, in the case of PBr, the first-stage decomposition rate is more intense than in the case of PN.

5.2. The kinetics of FF decomposition in oxidative and inert media investigated by the DMSTA method

Figures 4(a, b) demonstrates the results of studying the decomposition kinetics of the same specimen of PBr, consecutively obtained by the DMSTA method at a high heating rate, time dependences of the mass peak intensities of the decomposition products, proportional to their evolution rates, and temperature. Fig. 4 (a) refers to decomposition of PBr in inert medium (argon) with char formed. Fig. 4 (b) refers to oxidation of char in air, formed in decomposition in argon. The data on the kinetics of decomposition of PBr in air are shown in Fig. 5. Mass peaks 18, 31, 44 correspond to H_2O, C_2H_5OH and CO_2. For thermal decomposition of FF in air, three stages of FF transformation were identified for the mass peak intensity profiles: 1) the stage of drying with water vapour formed in the temperature range ΔT=50~300 °C with the maximum reaction rate at T_{max}~180 °C; 2) the formation stage of the volatile decomposition products (mass peak with m/e 31), including CO_2 and H_2O (ΔT=250~600 °C, T_{max}~450 °C). The mass spectra also contain hydrocarbons with mass peaks of m/e 15, 26, 27, 30, 39 not shown in the figure; 3) the char oxidation stage with CO_2 yielded (ΔT=600~800 °C, T_{max}~700 °C).

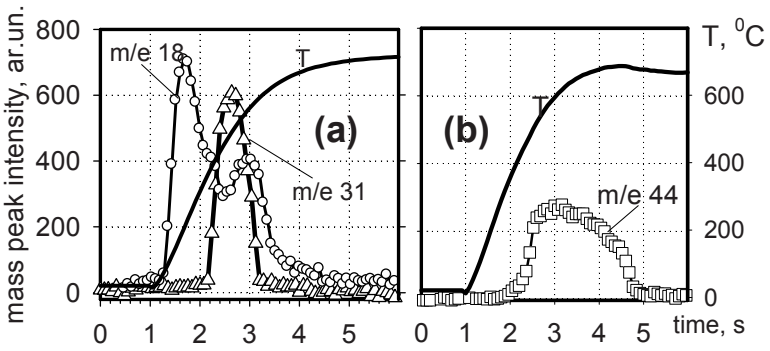

Fig. 4. Thermal decomposition of PBr powder at a high heating rate: a) in argon; b) char of PBr in air.

The kinetic parameters of thermal decomposition of FF were calculated using the mass peak intensity profile of m/e 31. We determined the kinetic parameters of thermal decomposition of FF by the method described in [19].

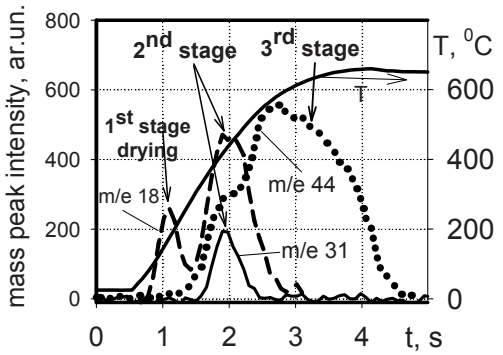

Fig. 5. Thermal decomposition of the powder of PBr at high heating rate in air.

Shown in Fig. 6 and in Table 2 are the rate constants of the decomposition reaction of FF in oxidative (A) and inert (B) media, obtained in this study at different heating rates (~150 K/s - DMSTA, a high heating rate; 0.17 K/s – TGA, a low heating rate), and some literature data.

The data of Fig 6, A (curves 1, 2) for the rate constant relating to the second stage of decomposition of PBr and PB at a high heating rate (DMSTA) have higher values than those relating to the second stage (lines 5, 6, 7) for the same FF specimens and the same decomposition stage at a low heating rate (TGA), although their activation energy values are close. The decomposition rate constants of stage 2 are 10/100 times higher than the decomposition rate constant of stage 3 at a high/low heating rate. The studies [4] for wood (pine) in stage 2 demonstrated a somewhat higher activation energy (~118

kJ/mol) but for the absolute value they are close to the data obtained in our study by the DMSTA method. It was found in our study that in the case of a high heating rate the decomposition rate constants both for stage 2 and 3 are significantly higher than in the case of a low heating rate.

Comparison of data for inert and oxidative media has shown the decomposition rate constant at stage 2 in the oxidative medium (lines 5A, 6A, 7A) to be higher than the decomposition rate constant in inert medium (lines 4B, 5B, 6B) at a low heating rate but lower at a high heating rate (lines 1A, 2A and lines 1B, 2B, respectively). The data of study [4] for wood (pine) for stage 2 in inert medium are closer to those obtained in our study at a high heating rate. The disagreement observed may be related to different types of FF.

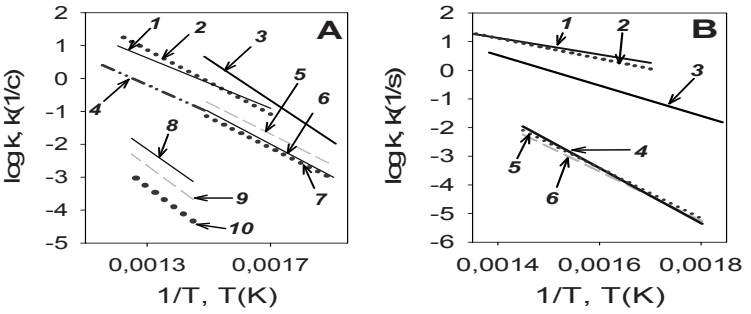

Fig. 6. The rate constants of the thermal decomposition reaction of FF in oxidative (A) and inert (B) media, obtained at different heating rates (~150 K/s – the DMSTA method, a high heating rate; 0.17 K/s – the TGA method, a low heating rate). The notations in Fig. 6A are used for the following: 1A, 2A – DMSTA, air, stage 2 for pine bark and branches; 3A – TGA, air, stage 2, wood (pine) [4]; 4A - DMSTA, air, stage 3, char of pine branches; 5A, 6A, 7A – TГA, He+21% O_2, stage 2 for pine needles, bark and branches; 8A, 9A, 10A – TГA, He+21% O_2, stage 3 for pine bark, needles and branches. The notations in Fig. 6B are used for the following: 1B, 2B – DMSTA, argon, stage 2 for pine bark and branches; 3B – TGA, nitrogen, stage 2, wood (pine) [4]; 4B, 5B, 6B – TGA, helium, stage 2 for pine bark, branch and needles.

Table 2. Kinetic parameters of the FF decomposition reaction in inert and oxidative media, obtained at different heating rates (150 K/s and 0.17 K/s)

	dT/dt, K/s	Inert / He+21% O_2 (step 2) / He+21% O_2 (step 3) / Air (step 2) / Air (step 3)		
		log k_0, k_0 (1/s)	E_a (kJ/mol)	Line on Fig. 6
PB	150	5.2/-/-/5.6/-	55.6/-/-/73.1/-	1B/-/-/1A/-
	0.17	12/6.4/6.4/-/-	184.3/94.5/125.8/-/-	4B/6A/8A/-/-
PBr	150	6.1/-/-/7.2/-	68.1/-/-/93.2/-	2B/-/-/2A/-
	0.17	10.6/5.8/5.8/-	167.6/89/133.7/-	5B/7A/10A/-/-
PN	0.17	10.2/6.3/6.3/-/-	164.3/89.9/131.7/-/-	6B/5A/9A/-/-
Char of PBr	150	-/-/-/-/5.2	-/-/-/-/79.4	-/-/-/-/4A
Wood (pine) [4]	0.34	8/9/-/-/-	101.5/118.6/-/-/-	3B/3A/-/-/-

5.3. Kinetic analysis of the thermal decomposition of forest fuels in helium/oxygen using the multi-component devolatilization mechanism

Thermal decomposition of forest fuels in oxidative atmosphere shows two major stages (except of the dehydration step): oxidative degradation of main components and oxidation of char formed [21]. Orfao et al. [22] studied thermal decomposition behavior of cellulose, xylan (representative of hemicellulose) and lignin under nitrogen and air by TGA. Cellulose decomposition rate exhibits a second peak at higher temperatures in air due to char oxidation, when compared with that in nitrogen. Hemicellulose decomposition process in air is also possible to define two zones. The rate of lignin decomposition process shows only one peak in air, but the processes of volatile formation and residue gasification occur simultaneously in the temperature range considered. So, the decomposition behavior of main biomass components reveals that biomass first loses its weight in pyrolysis, and then in oxidation when heating in air. Fig. 7 presents the mass loss rates of the bark, branch and needle samples at different heating rates in the 79% He+21% O_2 atmosphere by TGA. It is obvious

that the curves show two major mass loss processes, which correspond to the oxidative degradation of main components and oxidation of char. The first process also contains some sub-processes. For example, the curves of the bark samples in the first major process present a mass loss peak with a shoulder, which is similar to the mass loss process of the comparable temperature range in nitrogen. It is inferred that hemicellulose and cellulose decompose in this process. Though some research modeled the major mass loss process as a global reaction [21, 23, 24], it is not appropriate for the samples in Figure 7. In this paper, the mass loss process of forest fuels is modeled by four parallel reactions, nominally corresponding to the decomposition of three main components of biomass (hemicellulose, cellulose and lignin) and char oxidation.

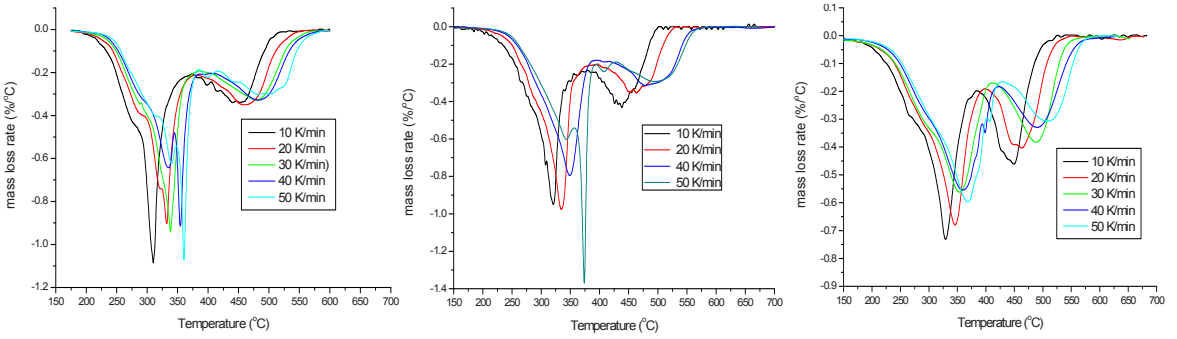

Fig. 7. Mass loss rates of forest fuel samples at different heating rates in the 79% He+21% O_2 atmosphere by TGA (A: PB; B: PBr; C: PN).

The overall conversion rate of forest fuel in helium/oxygen is described by the sum of the conversion rates of four pseudo reactions,

$$\frac{d\alpha}{dT} = \sum_{i=1}^{4} c_i \frac{d\alpha_i}{dT} \tag{1}$$

where c_i is the proportion of pseudo reaction i and $\sum_i r_i = 1$. The conversion α is defined as

$$\alpha = \frac{m_0 - m}{m_0 - m_\infty} \tag{2}$$

Here m is sample weight recorded by TGA, and m_0 the initial weight of sample, m_∞ the final weight of sample. Therefore the mass loss rate of sample can be expressed as

$$\frac{dm}{dT} = -(m_0 - m_\infty)\sum_{i=1}^{4} c_i \frac{d\alpha_i}{dT} \tag{3}$$

For each pseudo reaction, it is often that an irreversible first-order reaction models is assumed. That is, the conversion rate is described by

$$\frac{d\alpha_i}{dT} = \frac{A_i}{\beta}\exp(-\frac{E_i}{RT})(1-\alpha_i)^{n_i} \tag{4}$$

The simultaneous determination of the kinetic parameters for each reaction, and therefore determination of Eq. (3), was performed by minimizing the S_{DTG} coefficient of the experimental data (T, $d\alpha/dT$),

$$S_{DTG} = \sum_j S_j = \sum_j \sum_k [(dm/dT)^{\exp} - (dm/dT)^{simu}]^2 \quad (5)$$

where the superscripts of "*exp*" and "*simu*" are the experimental and simulated values. j is the number of experimental curves and k is the number of data points of each experimental curve. The minimization of S_{DTG} was carried out with the Levenberg–Marquardt non-linear fitting algorithm by Matlab software.

One parameter, Dev, is proposed to evaluate the deviation between the experimental and calculated curves as follows,

$$Dev = \frac{\sqrt{S_{DTG}/(jk)}}{\max[-(dm_j/dT)^{\exp}]} \quad (6)$$

This parameter can reflect the matching performance of the experimental and simulated curves.

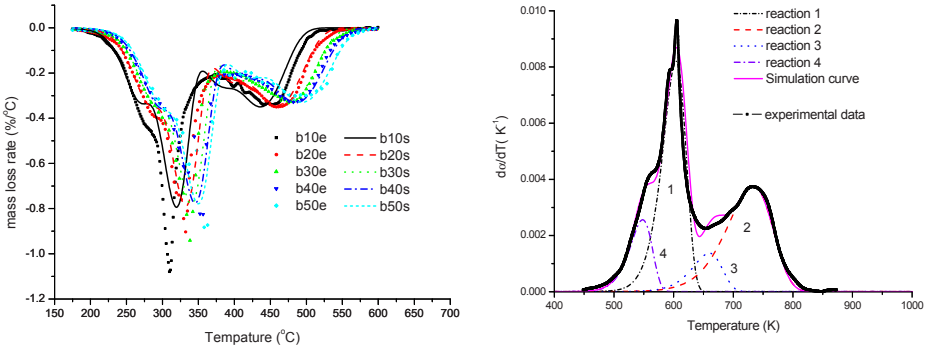

Fig. 8 (left). The experimental and simulated mass loss rate curves for bark in the 79% He + 21% O_2 atmosphere. ("b10e" means experimental data at 10K/min, "b10s" means simulated data at 10K/min); (right). The contribution of each reaction in bark decomposition process at 20 K/min in the 79% He + 21% O_2 atmosphere.

The result of modeling the mass loss process of bark by four parallel reactions is presented in Fig. 8-left. It is shown that the simulation curves agree with the experimental curves in the second major loss process very well while they predict lower values in the first major loss process. The sharp mass loss peaks of the experimental curves in the first major loss process seem smoothed by the model. For a clearer layout, the right-hand side of Fig. 8 presents the results at the heating rate of 20 K/min. In this figure, the curve values of $d\alpha/dT$ are calculated by the mass loss rate curve of dm/dT by differentiating Eq. (2). This figure also presents the contribution of each reaction to the simulation curve. It is found that reactions 1 and 2 play important roles in the decomposition process.

Table 3. Kinetic parameters for forest fuels decomposed in the 79 % He+21 % O_2 atmosphere

Sample	Pseudo-component	E (kJ/mol)	log$A$ (log s^{-1})	n (preset reaction order)	c (proportion)	Dev
PB	1	152.22	11.38	1	0.419	1.9%
	2	113.36	6.00	1	0.368	
	3	140.80	9.25	1	0.089	
	4	131.32	10.75	1	0.124	
PBr*	1	156.37	11. 70	1	0.436	1.8%
	2	88.94	4.25	1	0.441	
	3	149.13	12.19	1	0.094	

PN	4	94.29	7.47	1	0.029	2.4%
	1	130.95	9.14	1	0.439	
	2	115.16	6.08	1	0.382	
	3	107.45	8.20	1	0.147	
	4	63.37	4.65	1	0.032	

* Only the data at 10, 20, 40 K/min are used.

5.4. The structure of diffusion flame during combustion of a single pine branch in air

Pine branches (fall) were used in the experiments, with the diameter of 3-4 mm and about 4 cm long, dried at the temperature of 90 °C during 12 hours. Wet branches did not burn.

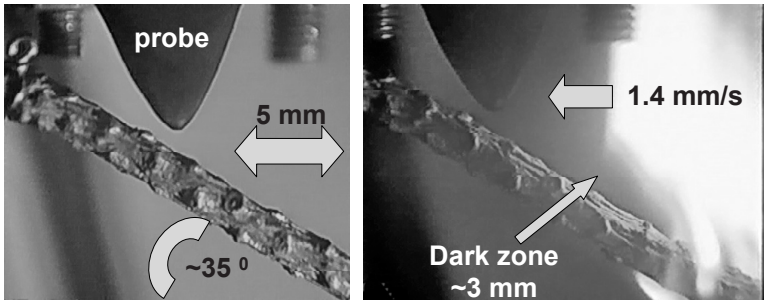

Fig. 9. The schematic of the experiment to study the structure of the diffusion flame of a PBr in air by the MBMS method.

Application of the GC/MS method allowed us to identify the following species among the thermal decomposition products of pine branches powder in argon at a high heating rate: ethanol (31, 45, 29, 27, 26), acetone (43, 15), and furan (39). The figures in brackets indicate the most intense mass peaks of these substances. In burning of the pine branch in the air the mass-spectrometric method identified the same peaks as in decomposition of the PBr powder.

The schematic of the experiment is shown in Fig. 9. The experiments were conducted in two variants. In the first case, the probe was not moved in relation to the branch. As the flame front moved at the velocity of about 1.4 mm/s along the branch fixed at an angle about 35 grad, time dependences of the intensities of mass peaks were obtained for the final and intermediate combustion products near the branch surface at the distance of ~1.5 mm, which are shown in Fig. 10. As the "dark" flame zone (oxygen concentration was close to zero) passed the sampling point (from 0 to 40 s), smooth increase of the mass peak intensities of hydrocarbon products (furan, acetone and ethanol) was observed, followed by their smooth decrease. In this flame zone, high concentrations of CO_2 and H_2O were measured. Then, during the time lapse from 40 to 70 s, the video recording showed slow combustion of char in air (oxygen presence is seen in Fig. 10) with a large amount of carbon dioxide, a small amount of water and ash formed. CO_2 concentration during combustion of char (time 40-70 s in Fig. 10) in the presence of sufficient amount of oxygen is the same as in the dark flame zone in its absence (0-40 s). Shown in Fig. 11 are the mass-spectra of the products in the zone located at the distance of ~1.2 mm from the burning surface of the PBr (dark zone), mainly of the volatile PBr pyrolysis products and of the combustion products at the distance of 4.5 mm (luminous zone) from the branch surface in the diffusion flame in air atmosphere. Oxygen was not found in significant amounts both near and far from the burning branch. In the second type of the experiments, the probe was first at the distance of ~ 4-5 mm from the branch surface. As flame passed in the space between the probe and the branch, the branch moved in the direction of the probe, thus allowing the structure of the diffusion flame from the zone of the final combustion products to the zone of products evolved from the burning surface. Dependence of the measured mass peak intensities on the distance from the burning surface of PBr is shown in Fig. 12. The width of the consumption zone of hydrocarbons like furan (m/e 39), acetone (m/e 43), and ethanol (m/e 27, m/e 31) during combustion of the pine branch in air was 0.8 mm.

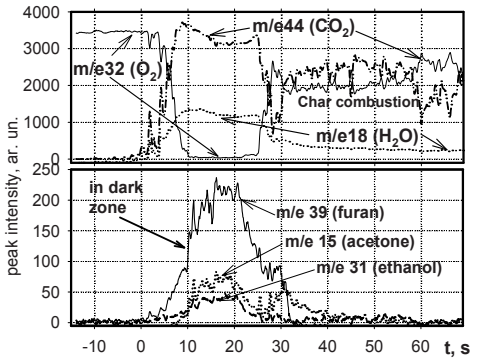

Fig. 10. Time dependence of mass peak intensities of the final and intermediate combustion products near the PBr surface at the distance of ~1.5 mm as flame passes the sampling point of the probe.

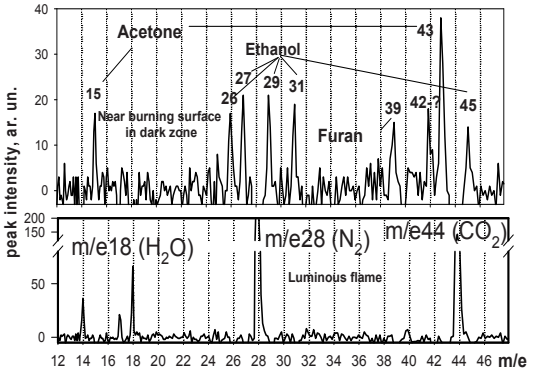

Fig. 11. Mass-spectra of the products in the zone at the distance of ~1.2 mm from the burning surface of the PBr (above) and of the combustion products at the distance of 4.5 mm from the combustion surface in air (below).

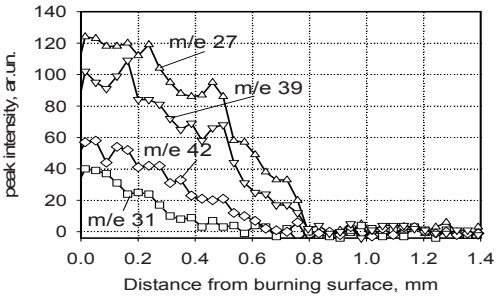

Fig. 12. The structure of the diffusion flame of a PBr when burnt in air.

6. Conclusions

The kinetics of pyrolysis and combustion of the Siberian forests fuels was studied at high heating rates (150 K/s) by the method of differential mass-spectrometric thermal analysis (DMSTA) *in situ,* using probing molecular-beam mass spectrometry and at low heating rates (0.17 K/s) by the thermogravimetric method. The kinetic parameters of SFF pyrolysis have been determined for oxidative and inert media for all stages of pyrolysis and simulation of SFF pyrolysis has been conducted using the multi-component devolatilization mechanism. It was found that in the case of a high heating rate the decomposition rate constants of pyrolysis are significantly higher than in the case of a low heating rate. Comparison of data for inert and oxidative media has shown the decomposition rate constant at stage 2 in the oxidative medium to be higher than the decomposition rate constant in inert medium at a low heating rate but lower at a high heating rate. The flame structure of a pine branch has been studied by probing molecular-beam mass spectrometry. Key species, ethanol, acetone and furan, have been detected both in the dark flame zone and in the pyrolysis products at high heating rates.

Acknowledgement

This work was partly supported by the Siberian Branch of Russian Academy of Sciences under grant No. 49, partly by the Russian Foundation for Basic Research under grant No. 13-03-91164 and by the the National Basic Research Program of China (973 Program, No. 2012CB719702), and National Natural Science Foundation of China under Grant 51120165001.

References

[1] Lautenberger, C. H., Fernando-Pello, C., 2009. A Model for the Oxidative Pyrolysis of Wood, Combustion and Flame 156, p. 1503.
[2] Font, R., Conesa, J. A., Molto, J., Munoz, M., 2009. Kinetics of Pyrolysis and Combustion of Pine Needles and Cones, Journal of Analytical and Applied Pyrolysis 85, p. 276.
[3] Shen, D. K., Gu, S., Luo, K. H., Bridgwater, A. V., Fang, M. X., 2009. Kinetic Study on Thermal Decomposition of Wood in Oxidative Environment, Fuel 88, p. 1024.
[4] Shen, D. K., Gu, S., Baoseng, Fang, M. X., 2011. Thermal Degradation Mechanisms of Wood under Inert and Oxidative Environments Using DAEM Methods, Bioresource Technology 10, p. 2047.
[5] Safi, M. J., Mishra, I. M., Prasad, B., 2004. Global Degradation Kinetics of Pine Needles in Air, Thermochemical Acta 412, p. 155.
[6] Leoni, E., Cancellieri, D., Balbi, N., Bernardini, A. F., Kaloustian, J., Marcelli, T., 2003. Thermal Degradation of Pinus Pinaster Needles by DSC, Part 2: Kinetics of Exothermic Phenomena, Journal of Fire Sciences 21, p.117.
[7] Liu, N. A., Fan, W., Dobashi, R., Huang, L., 2002. Kinetic Modeling of Thermal Decomposition of Natural Cellulosic Materials in Air Atmosphere, Journal of Analytical and Applied Pyrolysis 63, p. 303.
[8] Grishin, A. M., Sinitsyn, S. P., Akimova, I. V., 1991. Comparative Analysis of Thermokinetic Constant of Drying and Pyrolysis of Forest Fuels, Combustion and Explosion Physics Journal 27, p.17.
[9] Statheropoulos, M., Liodakis, S., Tzamtzis, N., Pappa, A., Kyriakou, S., 1997. Thermal Degradation of Pinus Halepensis Pine-needles Using Various Analytical Methods, Journal of Analytical and Applied Pyrolysis 43, p. 115.
[10] Leoni, E., Tomi, P., Khoumeri, B., Blabi, N., 2001. Thermal Degradation of Pinus Pinaster Needles by DSC. Part 1: Dehydration Kinetic, Journal of Fire Sciences 19, p. 379.
[11] Senneca, O., 2007. Kinetics of Pyrolysis, Combustion and Gasification of Three Biomass Fuels, Fuel Processing Technology 88, p. 87.
[12] Haykiri-Acma, H., Yaman, S., 2007. Interpretation of Biomass Gasification Yields regarding Temperature Intervals under Nitrogen–steam Atmosphere, Fuel Processing Technology 88, p. 417.
[13] Lin, Y-C., Cho, J., Tompsett, G. A., Westmoreland, P. R., Huber, G. W., 2009. Kinetics and Mechanism of Cellulose Pyrolysis, Journal of Physical Chemistry C 113, p. 20097.
[14] Shen, D. K., Gu, S., Luo, K. H., Bridgwater, A. V., Fang, M. X., 2009. Kinetic Study on Thermal Decomposition of Wood in Oxidative Environment, Fuel 88, p. 1024.
[15] Senneca, O., Chirone, R., Salatino, P., 2004. Oxidative Pyrolysis of Solid Fuels, Journal of Analytical and Applied Pyrolysis 71, p. 959.
[16] Korobeinichev, O. P., 1987. Dynamic Flame Probe Mass Spectrometry and Condensed-systems Decomposition, Combustion Explosion and Shock Waves 5, p. 64.
[17] Bodoev, N. V., Korobeinichev, O. P., Denisov, S. V., Paletsky, A. A., 1990. Investigation of Fast Heating Pyrolysis of Sapropelitic Coals by Mass-Spectrometrec Thermal Analysis, Journal Thermal Analysis 36, p. 481.
[18] Korobeinichev, O. P., Paletsky, A. A., Kuibida, L. V., Gonchikzhapov, M. B., Shundrina, I. K., 2013. Reduction of Flammability of Ultrahigh-molecular-Weight Polyethylene by using Triphenyl Phosphate Additives, Proceedings of the Combustion Institute 34, p. 2699.
[19] Paletsky, A. A., Budachev, N. V., Korobeinichev, O. P., 2009. Mechanism and Kinetics of the Thermal Decomposition of 5-Aminotetrazole, Kinetics and Catalysis 50, p. 627.
[20] Park, J. W., Oh, S. Ch., Lee, H. P., Kim, H. T., Loo, K. O., 2000. A Kinetic Analysis of Thermal Degradation of Polymers using a Dynamic Method, Polymer Degradation and Stability 67, p. 535.
[21] Chen, H. X., Liu, N. A., and Fan, W. C., 2006. Two-Step Consecutive Reaction Model and Kinetic Parameters Relevant to the Decomposition of Chinese Forest Fuels, Journal of Applied Polymer Science 102, p. 571.
[22] Orfao, J. J. M., Antunes, F. J. A., and Figueiredo, J. L., 1999. Pyrolysis Kinetics of Lignocellulosic Materials - Three Independent Reactions Model, Fuel 78, p. 349.
[23] Momoh, M., Eboatu, A. N., Kolawole, E. G., and Horrocks, A. R., 1996. Thermogravimetric Studies of the Pyrolytic Behaviour in Air of Selected Tropical Timbers, Fire and Materials 20, p. 173.
[24] Senneca, O., Chirone, R., and Salatino, P., 2002. A Thermogravimetric Study of Nonfossil Solid Fuels. 2. Oxidative Pyrolysis and Char Combustion, Energy & Fuels 16, p. 661.